# ACCURATE INTEGRAL TRANSFORM RESULTS FOR NATURAL CONVECTION IN A SQUARE CAVITY AT HIGH RAYLEIGH NUMBER

**Marco Aurélio Leal** – maleal@cnen.gov.br
**Jesús Salvador Pérez Guerrero –** jperez@cnen.gov.br
Comissão Nacional de Energia Nuclear, Coordenação de Rejeitos Radioativos – COREJ
Rua General Severiano, 90 – Botafogo
Rio de Janeiro – RJ - 22294.900– Brazil

***Abstract.*** *The classical thermally driven square cavity problem, with adiabatic top and bottom walls, offers challenging test cases for the co-validation of numerical methods. In this work, the laminar steady-state streamfunction-only formulation of the flow equations and the associated energy equation, under Boussinesq approximation, is employed to obtain accurate results through Generalized Integral Transform Techinique (GITT) for high Rayleigh numbers, where the very desirable hybrid characteristics of the GITT are explored in a situation of strong non-linear effects. Results will be presented for two different values of the Rayleigh number,* $10^6$ *and* $10^7$*, always for Prandtl number equal 0.71, and critical comparisons against previously reported benchmark solutions will be then performed.*

***Key Words:*** *Natural convection, Integral transform, Hybrid method*

## 1. INTRODUCTION

Laminar natural convection within square cavities, subjected to differentially heated vertical walls and insulated horizontal surfaces is an interesting and permanent problem because the resulting coupled formulation of the flow and energy equations offers a sufficiently complete and complex model for evaluations on accuracy and performance of each individual numerical scheme proposed in heat and fluid flow, as well as for critical comparisons among the various alternatives. The establishment of reliable benchmark results, inside the stability limit, then becomes of major interest in allowing for critical comparisons among different scheme variants and computational implementation strategies. Within this context, at the last 20 years many important contributions have been done by many researchers. Among others references, the most relevant ones for the present work are the classical work of de Vahl Davis (1983), the works of Saitoh & Hirose (1989), Hortmann et al. (1990) and Le Quéré (1991). De Vahl Davis (1983) utilized the streamfunction-vorticity formulation of the flow equations, and adopted the finite differences method with a false transient technique to obtain solutions in the Rayleigh number range from $10^3$ to $10^6$. Non-conservative second order differencing was employed, and Richardson's extrapolation strategy was invoked to generate the final benchmark results. Saitoh & Hirose (1989) made use of the transient streamfunction-vorticity formulation as well, but with a non-conservative fourth order differencing scheme, reporting numerical results for Ra= $10^4$, $10^6$ and only graphical results for Ra= $10^7$ and $10^8$, Hortmann et al. (1990) employed the steady-state primitive variables formulation, and applied a multigrid finite volume scheme for solving the cases Ra= $10^4$, $10^5$ and $10^6$. Le Quéré (1991) preferred the transient primitive variables formulation, and through a pseudo-spectral method based on Chebyshev polynomials, reported results for Ra= $10^6$, $10^7$ and $10^8$.

Recently, a hybrid numerical-analytical approach, known as the Generalized Integral Transform Technique (GITT), mainly reviewed by Cotta (1993) and Cotta and Mikhailov (1997), has been progressively established as a powerful tool in benchmarking and engineering applications for linear and nonlinear diffusion and convection-diffusion problems, including heat and fluid problems formulated through the boundary layer and Navier-Stokes equations. More specifically it is worth mentioning the integral transform solutions of the Navier-Stokes equations under streamfunction-only formulation, for incompressible flow within cavities, Pérez Gurrero and Cotta (1992), and natural convection under Boussinesq approximation inside rectangular enclosures for both, transient and steady states, respectively Leal (1998) and Leal et al. (1999). Leal (1998) investigated the transient behavior of the phenomena for three different values of the Rayleigh number range from $10^3$ to $10^5$. Benchmark steady state results were presented by Leal at al. (1999) for Ra= $10^3$, $10^4$, $10^5$ and $10^6$. Fortran77 codes were utilized by Leal to perform the transient and steady state results. In addition, natural convection within porous rectangular enclosures was accurately solved through the integral transform method, Baohua and Cotta (1993).

The hybrid nature of this approach allows for the automatic global error control along the solution process, towards an user prescribed accuracy target, making it particularly suitable in obtaining reference results for test-problems, which can then be employed in the validation of purely numerical approaches. The aim of the present work is reproducing accurate results through GITT for high Rayleigh numbers in the classical problem of natural convection inside enclosures, in this case Ra=$10^6$ and $10^7$, always for Prandtl number equal 0.71. A Fortran 90 code was constructed and a new parametrization strategy was adopted in the computational algorithm to the solution of the transformed ODE system.

## 2. PROBLEM FORMULATION

Steady laminar natural convection of a Newtonian fluid inside a square enclosure is considered. The lateral walls are differentially heated, while the top and the bottom walls are kept insulated. The Boussinesq approximation for the buoyancy effect is invoked, and this coupled heat and fluid flow problem is formulated via vorticity transport equation in streamfunction-only formulation, and the associated energy equation, in dimensionless form as:

$$-\frac{\partial\psi}{\partial y}\frac{\partial(\nabla^2\psi)}{\partial x}+\frac{\partial\psi}{\partial x}\frac{\partial(\nabla^2\psi)}{\partial y}=-\Pr\nabla^4\psi+\Pr\,\mathrm{Ra}\,\frac{\partial T}{\partial x} \tag{1.a}$$

$$\frac{\partial\psi}{\partial y}\frac{\partial T}{\partial x}-\frac{\partial\psi}{\partial x}\frac{\partial T}{\partial y}=\nabla^2 T \tag{1.b}$$

with boundary conditions:

$$T=1\ ; \qquad \psi=\frac{\partial\psi}{\partial x}=0\ ; \qquad x=0 \tag{1.c-e}$$

$$T=0\ ; \qquad \psi=\frac{\partial\psi}{\partial x}=0\ ; \qquad x=1 \tag{1.f-h}$$

$$\frac{\partial T}{\partial y}=0\ ; \quad \psi=\frac{\partial\psi}{\partial y}=0\ ; \qquad y=0 \tag{1.i-k}$$

$$\frac{\partial T}{\partial y}=0\ ; \quad \psi=\frac{\partial\psi}{\partial y}=0\ ; \qquad y=1 \tag{1.l-n}$$

The remaining dimensionless variables are given by:

$$x=\frac{x_*}{L}\ ;\ \ y=\frac{y_*}{L}\ ;\ \ u=\frac{L}{\alpha}u_*\ ;\ \ v=\frac{L}{\alpha}v_*\ ;\ T=\frac{T_*-T_c}{T_h-T_c}\ ;\ \psi=\frac{\psi_*}{\alpha} \tag{2.a-f}$$

where "*" identifies the dimensional variables, $L$ is the cavity length, while $T_h$ and $T_c$ are the uniform temperatures at hot and cold walls. The Rayleigh and Prandtl numbers are defined, respectively by:

$$\mathrm{Ra}=\frac{g\,\beta\,(T_h-T_c)\,L^3}{\alpha\,\nu} \quad \text{and} \quad \mathrm{Pr}=\frac{\nu}{\alpha} \tag{3.a,b}$$

where the associated equation operators are given by:

$$\nabla^2=\frac{\partial^2}{\partial x^2}+\frac{\partial^2}{\partial y^2} \quad ; \quad \nabla^4=\frac{\partial^4}{\partial x^4}+2\frac{\partial^4}{\partial x^2\partial y^2}+\frac{\partial^4}{\partial y^4} \tag{4.a,b}$$

## 3. SOLUTION METHODOLOGY

The integral transform approach is based on the eigenfunction expansion of the potentials, in this case, temperature and streamfunction. For this purpose, the boundary conditions on the coordinate variable to be eliminated through integral transformation, are first made homogenous, so as to coincide with the boundary conditions of the eigenvalue problem to be proposed. Thus, a filtering solution for the temperature field is developed, in the form:

$$T(x,y)=T^*(x,y)+T_p(x) \tag{5.a}$$

where the filter $T_p$ is the solution of the pure conduction problem in the cavity, readily obtained as:

$$T_p(x) = 1 - x \tag{5.b}$$

which results in producing a new temperature problem, for $T^*$, with homogenous boundary conditions, and the final filtered system is rewritten as:

$$\frac{\partial^4\psi}{\partial y^4} + 2\frac{\partial^4\psi}{\partial x^2\partial y^2} + \frac{\partial^4\psi}{\partial x^4} = \frac{1}{\Pr}\left[\frac{\partial\psi}{\partial y}\frac{\partial^3\psi}{\partial x^3} + \frac{\partial\psi}{\partial y}\frac{\partial^3\psi}{\partial y^2\partial x} - \frac{\partial\psi}{\partial x}\frac{\partial^3\psi}{\partial x^2\partial y} - \frac{\partial\psi}{\partial x}\frac{\partial^3\psi}{\partial y^3}\right] +$$

$$\text{Ra}\,\frac{\partial T^*}{\partial x} - \text{Ra} \tag{6.a}$$

$$\frac{\partial^2 T^*}{\partial y^2} + \frac{\partial^2 T^*}{\partial x^2} = \frac{\partial\psi}{\partial y}\frac{\partial T^*}{\partial x} + \frac{\partial\psi}{\partial x}\frac{\partial T^*}{\partial y} + \frac{\partial\psi}{\partial y} \tag{6.b}$$

with now homogeneous boundary conditions:

$$T^* = 0\ ; \quad \psi = \frac{\partial\psi}{\partial x} = 0\ ; \quad x = 0 \tag{6.c-e}$$

$$T^* = 0\ ; \quad \psi = \frac{\partial\psi}{\partial x} = 0\ ; \quad x = 1 \tag{6.f-h}$$

$$\frac{\partial T^*}{\partial y} = 0\ ; \quad \psi = \frac{\partial\psi}{\partial y} = 0\ ; \quad y = 0 \tag{6.i-k}$$

$$\frac{\partial T^*}{\partial y} = 0\ ; \quad \psi = \frac{\partial\psi}{\partial y} = 0\ ; \quad y = 1 \tag{6.l-n}$$

The next step is then the choice of the eigenfunctions for the dependent variables expansions. The "x" direction is selected to be eliminated through integral transformation, and the eigenvalue problem of biharmonic-type, previously studied in Pérez Guerrero et al. (1992), is adopted for the streamfunction representation. The related eigenfunctions are given by:

$$\tilde{X}_i(x) = \begin{cases} \cos\mu_i(x-1/2)\,sec(\mu_i/2) - \cos h\,\mu_i(x-1/2)\,sech(\mu_i/2)\,; \text{for } i = 1, 3, 5,... \\ sin\,\mu_i(x-1/2)\csc(\mu_i/2) - sinh\,\mu_i(x-1/2)\,csch(\mu_i/2)\,; \text{ for } i = 2, 4, 6,... \end{cases} \tag{7.a,b}$$

where the eigenvalues are obtained from the transcendental equation:

$$\tanh\frac{\mu_i}{2} = \begin{cases} -\tan(\mu_i/2) & \text{for } i = 1, 3, 5,\dots \\ \tan(\mu_i/2) & \text{for } i = 2, 4, 6,\dots \end{cases} \tag{8.a.b}$$

and the normalization integral is evaluated as unity, i.e., $N_i = 1$, for $i$= 1, 2, 3,....

For the temperature expansion, the classical second order diffusion operator yields a Sturm-Liouville-type problem, readily solved with the appropriate boundary conditions of first kind, at the lateral walls, to yield the eigenfunctions and the related eigenvalues as follows:

$$\phi_m(x) = sin\,\beta_m x \quad \text{and} \quad \beta_m = m\pi \;; \quad \text{for} \quad m = 1, 2, 3,... \tag{9.a,b}$$

and the norm evaluation yields:

$$M_m = 1/2 \;; \quad \text{for} \quad m = 1, 2, 3,... \tag{9.c}$$

The normalized eigenfunction $\tilde{\phi}_m$ then becomes:

$$\tilde{\phi}_p(x) = \frac{\phi_p(x)}{M_p^{1/2}} \tag{10}$$

The solution methodology proceeds towards the proposition of the integral transform pair for the potentials, the integral transformation itself and the inversion formula.

For the streamfunction field:

$$\overline{\psi}_i(y) = \int_0^1 \tilde{X}_i(x)\; \psi(x,y)\; dx, \qquad \text{transform} \tag{11.a}$$

$$\psi(x,y) = \sum_{i=1}^{\infty} \tilde{X}_i(x)\; \overline{\psi}_i(y), \qquad \text{inverse} \tag{11.b}$$

and for the temperature field:

$$\overline{T}_m(y) = \int_0^1 \tilde{\phi}_m(x)\; T^*(x,y)\; dx, \qquad \text{transform} \tag{12.a}$$

$$T^*(x,y) = \sum_{m=1}^{\infty} \tilde{\phi}_m(x)\; \overline{T}_m(y), \qquad \text{inverse} \tag{12.b}$$

The integral transformation process is now employed through operation of Eq.(6.a) with $\int_0^1 \tilde{X}_i(x)\,dx$ , to find the transformed streamfunction system:

$$\frac{d^4\overline{\psi}_i(y)}{dy^4} = \frac{1}{\Pr}\sum_{j=1}^{\infty}\sum_{k=1}^{\infty}\left[A_{ijk}\frac{d\overline{\psi}_j}{dy}\overline{\psi}_k + B_{ijk}\frac{d\overline{\psi}_j}{dy}\frac{d^2\overline{\psi}_k}{dy^2} - C_{ijk}\overline{\psi}_j\frac{d\overline{\psi}_k}{dy} - B_{ijk}\frac{d^3\overline{\psi}_j}{dy^3}\overline{\psi}_k\right] -$$

$$-\mu_i^4\overline{\psi}_i - 2\sum_{j=1}^{\infty} D_{ij}\frac{d^2\overline{\psi}_j}{dy^2} + \mathrm{Ra}\sum_{m=1}^{\infty} E_{im}\overline{T}_m - \mathrm{Ra}\;F_i\,, \qquad i = 1, 2, 3,... \tag{13}$$

Similarly, Eq.(6.b) is operated on with $\int_0^1 \tilde{\phi}_m(x)\,dx$ , to yield the transformed temperature problem:

$$\frac{d^2\overline{T}_m(y)}{dy^2} = \beta_m^2\overline{T}_m + \sum_{n=1}^{\infty}\sum_{j=1}^{\infty}\left[Q_{mnj}\overline{T}_n\frac{d\overline{\psi}_j}{dy} - S_{mnj}\frac{d\overline{T}_n}{dy}\overline{\psi}_j\right] - \sum_{j=1}^{\infty}P_{mj}\frac{d\overline{\psi}_j}{dy}\,,$$

$$m = 1, 2, 3,... \qquad (14)$$

Then, the resulting coupled infinite system of ordinary differential equations with boundary conditions at two points, for the transformed potentials, is described by Eqs.(13 and 14), together with the integral transformed boundary conditions:

$$\overline{\psi}_i(0) = 0\,; \quad \frac{d\overline{\psi}_i(0)}{dy} = 0\,; \quad \frac{d\overline{T}_m(0)}{dy} = 0 \qquad (15.a\text{-}c)$$

$$\overline{\psi}_i(1) = 0\,; \quad \frac{d\overline{\psi}_i(1)}{dy} = 0\,; \quad \frac{d\overline{T}_m(1)}{dy} = 0 \qquad (15.d\text{-}f)$$

The related coefficients $A_{ijk}$, $B_{ijk}$, $C_{ijk}$, $D_{ij}$, $E_{im}$, $F_i$, $Q_{mnj}$, $S_{mnj}$ and $P_{mj}$ are obtained analytically through Mathematica software system of symbolic manipulation, Wolfram (1991), and automatically generated in Fortran form. More details can be seen in Leal (1998), Leal et al. (1999) and Cotta and Mikhailov (1997).

## 4. COMPUTATIONAL PROCEDURE

For computational purposes, the expansions are truncated to *NV* and *NT* terms, respectively, streamfunction and temperature fields, towards the user prescribed accuracy target. A Fortran 90 code was constructed and implemented on a PC Pentium 266-128Mb. The subroutine DBVPFD from the IMSL Library (1989) was employed as the boundary value problem solver, with an automatic local relative error selected to be $10^{-4}$ (i.e. ±1 in the fourth significant digit). An air-filled square cavity (Pr= 0.71) is considered with Rayleigh numbers equals to $10^6$ and $10^7$. An artificial parametrization over the source term in Eq. (15), controlled by the user, was performed in order to achieve convergence to the four significant digits required.

Once the transformed potentials, $\overline{\psi}_i$ and $\overline{T}_m$, have been numerically evaluated under controlled accuracy, the inversion formula, together with the filtering solution, are recalled to provide explicit analytical expressions, in the "y" direction, for the original potentials $\psi(x,y)$ and $T(x,y)$.

For comparison purpose two different definitions of Nusselt numbers are employed, as in the related literature. The maximum (or minimum) Nusselt number at the hot wall ($x$=0), is determined from the expression below:

$$Nu = -\frac{\partial T}{\partial x}\bigg|_{x=0} \qquad (16.a)$$

which is analytically represented after invoking the inversion formula (12.b) and the filtering solution, Eqs.(5.a,b), to yield:

$$Nu = -\left\{ \left[ \sum_{m=1}^{NT} \frac{d\tilde{\phi}_m(x)}{dx} \overline{T}_m(y) \right] + \frac{dT_p(x)}{dx} \right\}_{x=0} \tag{16.b}$$

And the overall average Nusselt number a cross-section is obtained from de Vahl Davis (1983) as:

$$\overline{Nu} = \int_0^1 \int_0^1 \left[ u(x,y)T(x,y) - \frac{\partial T(x,y)}{\partial x} \right] dx\, dy \tag{17}$$

The integrations required in Eq. (17) were numerically performed by making use of the appropriate subroutines in the IMSL Library (1989).

## 5. RESULTS AND DISCUTION

For low values of Rayleigh number, full convergence to four digits can be achieved at quite low truncation orders. As this parameter is increased, the inertia and convection terms which act as source functions within the proposed diffusion-based expansions, gain relative importance and, as typical in this type approach, slow to a certain extent convergence rates. Thus, for severe cases as Ra= $10^6$ and $10^7$, the user requested precision limit is reached at the expense of additional computational effort, as the truncation orders are increased further by the algorithm.

Table 1 brings some comparison of the present integral transform results against previously reported benchmark results, obtained through different approaches. The following values were employed in these comparative table:

$|\psi_{MED}|$ - streamfunction modulus at the cavity center ($x = y = 1/2$).

$|\psi_{MAX}|$ - maximum streamfunction modulus and respective location $x$ and $y$.

$\overline{Nu}$ - overall average Nusselt number across the cavity.

It should be observed in Table 1 an excellent agreement between the results presented through integral transform and those reported by other referred authors. At Ra=$10^6$, a fully coincidence can be noted against Le Quéré (1991) and GITT results. For the case of Ra=$10^7$, some scattering among the solution methodologies becomes more apparent, confirming the simulation difficulties encountered in this situation of high Rayleigh number.

The convergence behavior of the local Nusselt number along the hot wall (x=0), for different truncation orders, is illustrated in Figure 1. It can be observed that in the situation of Ra= $10^6$ the convergence processes is completely achieved with $NV$=$NT$=50 terms. Even in the more severe case of Ra= $10^7$ the convergence is attained in positions above $y$=0.05 with $NV$=$NT$=60 terms. It is noticeable that the necessity of highest truncation orders can be just motivated by the convergence behavior in regions very close by the bottom wall.

Tables 2 and 3, respectively Ra= $10^6$ and $10^7$, show temperature values at different positions within the cavity, for increasing pairs of truncation order $NV$/$NT$. It should be noticed that the user requested precision limit of ±1 in the fourth significant digit is reached in all selected positions for Ra= $10^6$, unless in the opposite corners at $x$=$y$=0.1 and $x$=$y$=0.9. Table 3,

Table 1. Comparison of the cavity center stream function, maximum stream function and global Nusselt number for the two different values of Ra with available results.

| Ra | $\lvert\psi_{MED}\rvert$ | $\lvert\psi_{MAX}\rvert$ (x / y) | $\overline{Nu}$ |
|---|---|---|---|
| **$10^6$** | | | |
| GITT - Present work | 16.39 | 16.81 (0.15/0.55) | 8.825 |
| De Vahl Davis (1983) | 16.32 | 16.75 (0.151/0.547) | 8.800 |
| Saitoh & Hirose (1989) | 16.379 | - | 8.7956 |
| Hortmann et al.(1990) | - | - | 8.8251 |
| Le Quéré (1991) | 16.386 | 16.811 (0.150/0.547) | 8.825 |
| **$10^7$** | | | |
| GITT - Present work | 29.33 | 30.12 (0.09/0.55) | 16.52 |
| Le Quéré (1991) | 29.36 | 30.16 (0.086/0.556) | 16.523 |

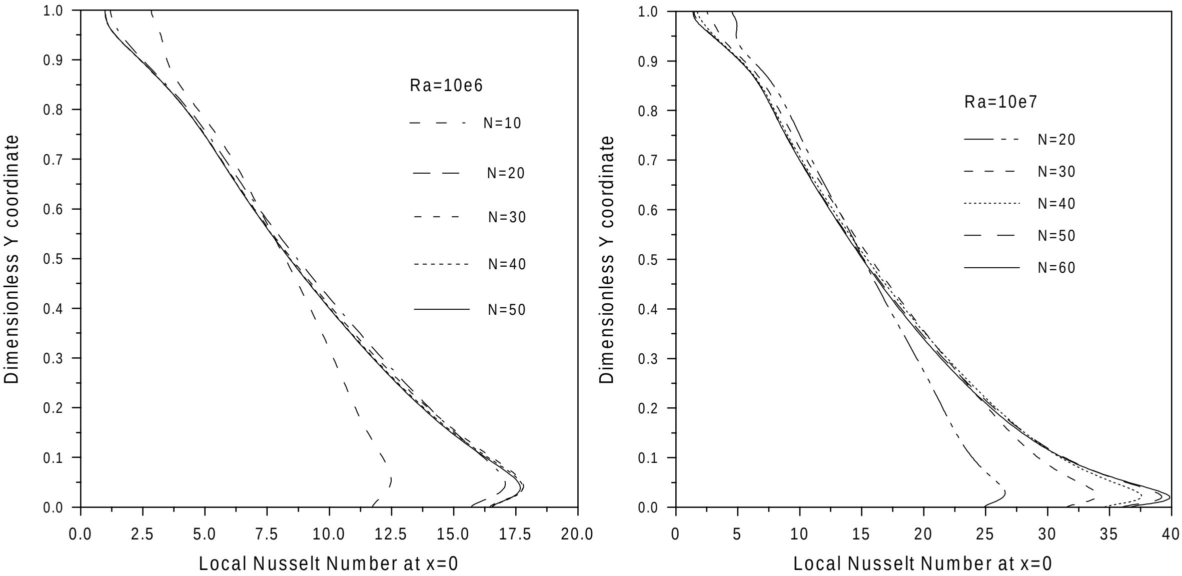


(a) (b)

Figure 1. The convergence behavior of the local Nusselt number along the hot wall. (a) Ra= $10^6$, (b) Ra= $10^7$.

Table 2. Convergence of the temperature field (x$10^{-1}$) for $Ra = 10^6$.

| ***Ra* = $10^6$ ; *Pr* = 0.71** | | | | | | | | | |
|---|---|---|---|---|---|---|---|---|---|
| **NV/NT** | ***x*=0.1 *y*=0.1** | ***x*=0.1 *y*=0.5** | ***x*=0.1 *y*=0.9** | ***x*=0.5 *y*=0.1** | ***x*=0.5 *y*=0.5** | ***x*=0.5 *y*=0.9** | ***x*=0.9 *y*=0.1** | ***X*=0.9 *y*=0.5** | ***x*=0.9 *y*=0.9** |
| 10/10 | 2.373 | 4.880 | 7.743 | 2.238 | 5.000 | 7.762 | 2.257 | 5.120 | 7.627 |
| 20/20 | 2.226 | 4.782 | 8.013 | 1.791 | 5.000 | 8.209 | 1.987 | 5.218 | 7.774 |
| 30/30 | 2.199 | 4.793 | 8.028 | 1.762 | 5.000 | 8.238 | 1.972 | 5.207 | 7.801 |
| 40/40 | 2.187 | 4.791 | 8.026 | 1.761 | 5.000 | 8.239 | 1.974 | 5.209 | 7.813 |
| 50/50 | 2.192 | 4.791 | 8.027 | 1.762 | 5.000 | 8.238 | 1.973 | 5.209 | 7.808 |

shows a convergence of ±7 in the fourth digit for Ra= $10^7$ in the worst selected positions, *x*=*y*=0.1 and *x*=*y*=0.9, confirming some difficulty in reaching the prescribed convergence for very high Rayleigh numbers in regions very close by the vertical enclosure wall, what is related to thinner boundary layers, as can be illustrated in Figures 6 and 7.

Table 3. Convergence of the temperature field ($\times 10^{-1}$) for $Ra = 10^7$.

| ***Ra* = $10^7$ ; *Pr* = 0.71** | | | | | | | | | |
|---|---|---|---|---|---|---|---|---|---|
| **NV/NT** | ***x*=0.1 *y*=0.1** | ***x*=0.1 *y*=0.5** | ***x*=0.1 *y*=0.9** | ***x*=0.5 *y*=0.1** | ***x*=0.5 *y*=0.5** | ***x*=0.5 *y*=0.9** | ***x*=0.9 *y*=0.1** | ***x*=0.9 *y*=0.5** | ***x*=0.9 *y*=0.9** |
| 20/20 | 2.226 | 4.782 | 8.013 | 1.791 | 5.000 | 8.209 | 1.987 | 5.218 | 7.774 |
| 30/30 | 1.823 | 4.917 | 7.388 | 1.723 | 5.000 | 8.277 | 2.612 | 5.083 | 8.177 |
| 40/40 | 1.845 | 4.919 | 7.419 | 1.701 | 5.000 | 8.299 | 2.581 | 5.081 | 8.155 |
| 50/50 | 1.833 | 4.923 | 7.422 | 1.696 | 5.000 | 8.304 | 2.578 | 5.077 | 8.167 |
| 60/60 | 1.826 | 4.921 | 7.420 | 1.695 | 5.000 | 8.305 | 2.580 | 5.079 | 8.174 |

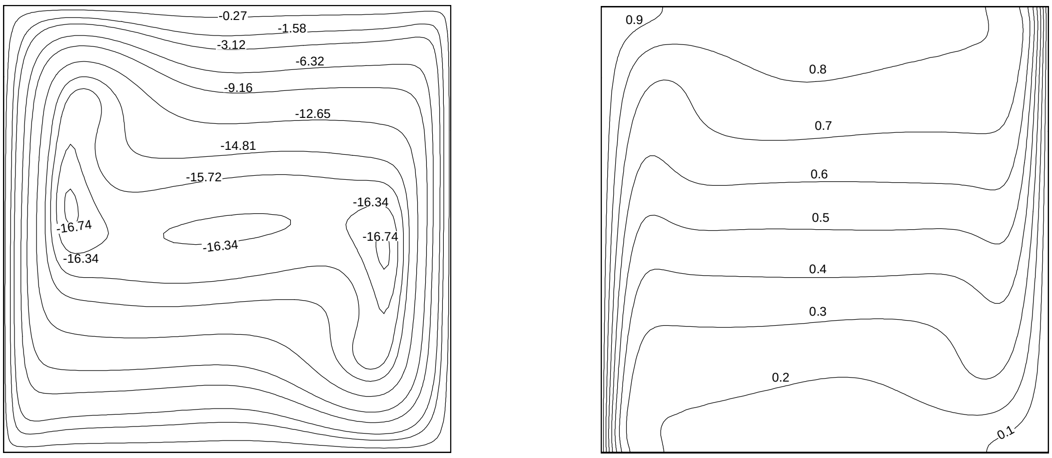


Figure 6- Streamlines and isotherms for $Ra=10^6$.

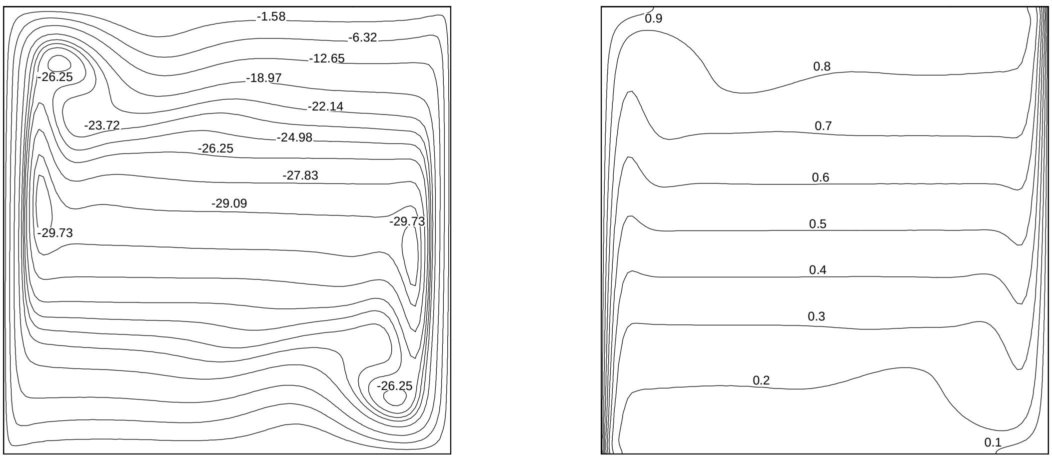


Figure 7- Streamlines and isotherms for $Ra=10^7$.

## 6. CONCLUSIONS

The Integral transform approach was successfully used to perform accurate results for high Rayleigh numbers, as $10^6$ and $10^7$. The utilization of a Fortran 90 code with a new parametrization strategy controlled by the user were fundamentals to attain the work purpose.

One can also verify that in the asymptotic limit of $Ra \rightarrow \infty$, the thermal layers into the cavity are characterized by vertical thermal boundary layers very close by the verticals walls, which difficult the convergence processes in these regions.

The next step is to make use of a supercomputer to achieve benchmark results for the very high Rayleigh number $10^8$.

***Acknowledgments***

The authors would like to acknowledge the financial support provided by CAPES/COFECUB, research sponsoring agencies in Brazil and France.

## REFERENCES

Baohua, C. and Cotta, R.M., 1993, Integral Transform Analysis of Natural Convection in Porous Enclosures, Int. J. Numer. Meth. in Fluids, vol. 17, pp. 787-801.

Cotta, R.M., 1993, Integral Transforms in Computational Heat and Fluid Flow, CRC Press, Boca Raton, FL.

Cotta, R.M. and Mikhailov, M.D., 1997, Heat Conduction: -Lumped Analysis, Integral Transform, Symbolic Computation, Wiley-Interscience, New York.

de Vahl Davis, G., 1983, Natural Convection of Air in a Square Cavity: A Bench Mark Numerical Solution, Int. J. Numer. Meth. in Fluids, vol. 3, pp. 243-264.

Hortmann, M., Peric, M. and Scheuerer, G., 1990, Finite Volume Multigrid Prediction of Laminar Natural Convection: Bench-Mark Solutions, Int. J. Numer. Meth. in Fluids, vol. 11, pp. 189-207.

IMSL Library, Math/Lib., Houston, TX 1989.

Le Quéré, P., 1991, Accurate Solutions to the Square Thermally Driven Cavity at High Rayleigh Number, Computers & Fluids, vol. 20, nº 1, pp. 29-41.

Leal, M.A., 1998, Natural Convection in Enclosures, in The Integral Transform Method in Thermal-Fluid Sciences & Engineering, ed. R.M. Cotta, Begell House Inc., NY.

Leal, M.A., Pérez Guerrero, J.S. and Cotta, R.M., 1999, Natural Convection Inside Two-Dimensional Cavities: - The Integral Transform Method, Commun. Numer. Meth. Engng., vol. 15, pp. 113-125.

Pérez-Guerrero, J.S. and Cotta, R.M., 1992, Integral Transform Method for Navier-Stokes Equations in Streamfunction-Only Formulation, Int. J. Numer. Meth. in Fluids, vol. 15, pp. 399-409.

Saitoh, T., and Hirose, K., 1989, High-accuracy Bench Mark Solutions to Natural to Convection in a Square Cavity, Computational Mechanics, vol. 4, pp. 417-427.

Wolfram, S., 1991, MATHEMATICA- A System for Doing Mathematics by Computer, The Advanced Book Program, Addison-Wesley Publishing Co., Redwood City, California, 1991.